THE BRIGHTEST AGB STARS IN THE INNER BULGE OF M31

T. J. Davidge [1]
Canadian Gemini Office, Herzberg Institute of Astrophysics,
National Research Council of Canada, 5071 W. Saanich Road,
Victoria, British Columbia, Canada V9E 2E7
email:tim.davidge@nrc.ca

ABSTRACT

JHK images with angular resolutions approaching the diffraction limit of the 3.6 meter Canada-France-Hawaii Telescope are used to investigate the bright AGB content of the M31 bulge. The AGB-tip in a field 2.6 arcmin from the galaxy center occurs at $K = 15.6$, which is significantly fainter than measured in previous ground-based studies that sampled similar projected distances from the center of M31, but were affected by crowding. Within 2.6 arcmin of the center of M31 the number density of bright AGB stars scales with r-band surface brightness, and the K brightness of the AGB-tip does not vary measureably with radius. It is concluded that the infrared bright AGB stars (1) belong to the bulge, and not the disk, and (2) are well mixed throughout the inner bulge, suggesting that they formed at a time when the overall structural properties of the M31 bulge were imprinted. The bolometric luminosity functions (LFs) of the M31 bulge and Baade's Window are in excellent agreement, while the brightest AGB stars in the M31 bulge, the Galactic bulge, and M32 have similar M_K. Barring a fortuitous tuning of age and metallicity to produce AGB-tips with similar brightnesses, it is suggested that the brightest stars in M32 and the bulges of M31 and the Milky-Way belong to an old, metal-rich population; these stars are bright not because they have a young or intermediate age, but because they have a high metallicity.

Subject headings: galaxies: individual (M31) - galaxies: stellar content - galaxies: bulges - stars: AGB and post-AGB

---

[1]Visiting Astronomer, Canada-France-Hawaii Telescope, which is operated by the National Research Council of Canada, the Centre National del la Recherche Scientifique, and the University of Hawaii

1. INTRODUCTION

As the nearest large external galaxy, M31 provides an unprecedented laboratory for probing galaxy evolution. The stellar content in the central few arc minutes of M31 provides a fossil record that can be used to trace the evolution of the bulge, and possibly even the origins of the super-massive black hole (Dressler & Richstone 1988; Kormendy 1988) and double nucleus (Lauer et al. 1993). Because of the obvious problems posed by high stellar densities, most studies of the stellar content near the center of M31 have relied upon integrated spectra. Bica, Alloin, & Schmidt (1990) used evolutionary synthesis techniques to conclude that the inner bulge of M31 is dominated by an old, metal-rich component, although signatures of an intermediate-age population contributing 10 – 20% of the visible light, and even a component with an age of a few Myr, were also found. Davidge (1997) used a grid of long-slit spectra to map the stellar content within 30 arcsec of the nucleus, and concluded that (1) younger, more metal-rich populations occur at smaller radii, (2) [Mg/Fe] varies with radius, in the sense that [Mg/Fe] decreases towards smaller radii, as expected if the youngest stars formed from material enriched by SN I, whereas the main body of the bulge formed from material enriched by SN II, and (3) the radial gradients in stellar content differ from those in the elliptical galaxies NGC 3379 and NGC 4472, where age and [Mg/Fe] appear not to change with radius. Sil'Chenko, Burenkov, & Vlasyuk (1998) conclude that the stars near the nucleus of M31 are three times younger than those in the surrounding bulge.

Studies of resolved stars provide a direct means of probing stellar content and checking the results from integrated spectra, although only the brightest objects can typically be observed, and data with high angular resolutions are required to overcome crowding. There is an absence of main sequence stars hotter than B0V (Bohlin et al. 1985) in the M31 bulge, although a large population of relatively faint hot stars is present in the UV images (Brown et al. 1998). While originally thought to be post-AGB objects (King et al. 1992, Ferguson & Davidsen 1993), it is more likely that these sources are evolving on the horizontal branch (Brown et al. 1998). Rich & Mould (1991), Davies, Frogel, & Terndrup (1991), Rich, Mould, & Graham (1993), Rich & Mighell (1995) Davidge et al. (1997), and Stephens et al. (2001a, b) studied the near-infrared properties of stars in various M31 bulge fields. Rich et al. (1989) find that the brightest giants in the M31 and Galactic bulges are spectroscopically similar, while Rich & Mould (1991) and Rich, Mould, & Graham (1993) conclude that the M31 bulge contains stars that are more luminous than the brightest stars in the Galactic bulge. Using J, H, and K observations obtained with NICMOS, Stephens et al. (20001b) investigated the stellar content in fields surrounding five metal-rich M31 globular clusters, and concluded that (1) the LF of the M31 bulge at near-infrared wavelengths is similar to that in Baade's Window (BW), and (2) there is no evidence for a significant population of

bright young stars. The existence of a very bright stellar component in the M31 bulge has long been questioned, and it has been argued that such a population could be an artifact of crowding (DePoy et al. 1993; Renzini 1998; Jablonka et al. 1999) or, at larger distances from the nucleus, contamination from disk stars (Davies et al. 1991), although Rich et al. (1993) conclude that disk contamination is not an issue for fields within 500 parcsecs of the galaxy center.

In the present paper high angular resolution J, H, and Ks images are used to investigate the brightness and spatial distribution of stars evolving on the upper portions of the AGB in two M31 inner bulge fields, with the goal of gaining insight into the nature and origin of the brightest stars in the M31 bulge. The paper is structured as follows. The observations and procedures used to reduce the data, as well as the methods used to measure stellar brightnesses, are discussed in §2. The stellar contents of the two fields are investigated in §3 and §4, while a summary and discussion of the results follows in §5.

2. OBSERVATIONS, DATA REDUCTION, & PHOTOMETRIC MEASUREMENTS

The data were recorded during two observing runs with the KIR imager and CFHT Adaptive Optics Bonnette (AOB; Rigaut et al. 1998). KIR contains a 1024×1024 Hg:Cd:Te detector, with each pixel subtending 0.034 arcsec on a side; hence, the total imaged field is 35×35 arcsec. The CFHT AOB uses natural guide stars as reference beacons, and contains a 19 element curvature wavefront sensor (WFS) and a 19 electrode deformable bimorph mirror. The signal from the WFS is sampled at a frequency of 1000 Hz. The system is operated with automatic mode gain optimization to adapt to guide star brightness and atmospheric conditions, and is designed to deliver diffraction-limited angular resolution at near-infrared wavelengths during median Mauna Kea seeing conditions; however, if the seeing degrades from its median value, or the guide star is faint, then the delivered FWHM is intermediate between the diffraction-limited and uncorrected cases.

A field 2.6 arcmin south west of the galaxy nucleus, centered on the $R = 13$ star GSC 02801–02015 (RA 00:42:45.1, DEC +41:13:31.3 E2000), which served as the reference source for AO compensation, was observed through J, H, and Ks filters on the night of UT September 5 1998. The total integration time was 20 minutes per filter, with five 60 sec exposures being recorded at each corner of a 0.5×0.5 arcsec square dither pattern. The seeing conditions were poor by Mauna Kea standards, and stars in the final images have very low Strehl rations, with FWHM = 0.35 arcsec. This field will be refered to as the 'bulge' field for the remainder of the paper.

The central field of M31 was observed through J, H, and Ks filters during the night of UT September 11, 2000, with the semi-stellar nucleus of M31 serving as the reference source for AO compensation. The exposure times and observing strategy were the same as those employed for the bulge field. The seeing conditions were much better than during the 1998 run, and stars in the final images have FWHM = 0.27 arcsec in J, 0.15 arcsec in H, and 0.17 arcsec in Ks; the diffraction pattern produced by the telescope optics is clearly evident in the point spread functions (PSFs) constructed from the H and Ks images. This field will be refered to as the 'central' field for the remainder of the paper.

The data were reduced using the procedures described by Davidge & Courteau (1999), which correct for dark current, flat-field variations, thermal emission along the optical path, and variability in the DC sky level. The final Ks images of both fields are shown in Figures 1 and 2.

The brightnesses of individual stars were measured with the PSF-fitting program ALLSTAR (Stetson & Harris 1988), using PSFs and star lists obtained from tasks in DAOPHOT (Stetson 1987). A single PSF was constructed for each image. While anisoplanicity causes the PSF to vary with distance from the reference source, past experience indicates that the use of a single PSF does not introduce large photometric uncertainties over the KIR field (e.g. Davidge & Courteau 1999; Davidge 2001). Aperture corrections were determined from growth curve analysis of the PSF stars after subtracting neighboring objects, and the estimated uncertainty in the aperture corrections is ± 0.05 magnitude. Both datasets were recorded during clear sky conditions, and the photometric calibration was determined from observations of UKIRT faint standard stars (Casali & Hawarden 1992). The brightnesses of the standard stars were measured using apertures established by growth curve analysis, and the uncertainties in the photometric zeropoints is $\pm 0.02 - 0.03$ mag.

Unresolved stars create a non-uniform background in both fields, which complicates efforts to measure local sky levels and obtain reliable photometry. This background was removed using the iterative technique described by Davidge, Le Févre, & Clark (1991). Background structure was mapped by applying a 2×2 arcsec running median filter to star-subtracted frames, and the result was subtracted from the images prior to obtaining a final set of photometric measurements. This procedure does not contribute additional random noise to the data because of the large smoothing kernel used to construct the background frame.

Artificial star experiments were used to estimate the uncertainties in the photometric measurements, calibrate systematic effects, which can be significant for stars near the faint limit of the data, and estimate incompleteness. The brightnesses of artificial stars

were measured using the same procedures that were applied to the actual data, including background subtraction. The artificial star experiments assume a single PSF for each field, and so do not account for anisoplanicity; however, the good agreement between the predicted and observed scatter in the bulge field CMDs (§3) confirms that anisoplanicity does not dominate the uncertainties in the photometry.

3. THE BULGE FIELD

3.1. The CMDs and Comparisons with Baade's Window

The $(K, H-K)$ and $(K, J-K)$ CMDs of the bulge field are shown in Figure 3. The uncertainties predicted from the artificial star experiments match the scatter in the data. Not only does this agreement lend confidence to the predictions made from the artificial star experiments, but it also indicates that random uncertainties in the photometric measurements, rather than star-to-star differences in intrinsic properties, are the main sources of scatter in these data.

The stars plotted in Figure 3 are evolving on the upper AGB. There is a locus of stars near the blue edge of the $(K, J-K)$ CMD that runs from $J-K = 1.4$ at $K = 16.4$ to $J-K = 1.6$ at $K = 15.6$; the $(K, H-K)$ and $(K, J-K)$ CMDs of the M32 outer field studied by Davidge (2000a) also show a well-defined sequence at the bright end. This sequence disappears near $K = 16.4$ in Figure 3, at which point the CMD broadens. This broadening is not due to the RGB-tip, as this feature occurs near $K = 18$ at the distance of M31.

The projected distance of the bulge field from the nucleus of M31 is 0.6 kpc, which is comparable to the projected separation between BW and the Galactic Center (GC). Frogel & Whitford (1987) studied the photometric properties of M giants in BW, and found that late M giants typically have $J-K \sim 1.3$ and $H-K \sim 0.4$. If shifted to the distance of M31, a late M giant from BW would have $K \sim 17$, and the colors of stars in the M31 bulge field at this brightness match the typical values for M giants in BW.

The peak brightness in the M31 bulge field is similar to that in BW. The brightest star in Figure 3 has $K = 15.4$, and is 0.3 mag brighter than the main body of the giant branch, which has $M_K = -8.7 \pm 0.1$ if $\mu_0 = 24.4$ (van den Bergh 2000); this distance modulus for M31 is adopted for the remainder of the paper. The brightest star in the Frogel & Whitford (1987) sample is number 239, which has $M_K = -9.5$, while star number 181, which is their second brightest object, has $M_K = -9$. The 0.5 mag gap in K between the brightest and second brightest star in the Frogel & Whitford compilation suggests that objects like star

239 may be rare, perhaps because they are long period variables viewed at the peak of their cycle. Consequently, if star 181 is adopted as a representative example of the bright stellar content in BW, then the peak K brightness in the M31 bulge field is similar to that in BW.

Frogel & Whitford (1987) derived $K-$band bolometric corrections for giants in BW as a function of $J-K$, and their calibration was applied to the M31 bulge field measurements to investigate the bolometric LF of stars in this field. The resulting LF, corrected for incompleteness using the results from the artificial star experiments, is shown in Figure 4. Also shown in this figure is the bolometric LF of BW, constructed from the entries listed in Table 1 of Frogel & Whitford (1987), but assuming a distance modulus of 14.5 (Reid 1993). The BW LF, which has been scaled to match the total number of stars in the M31 LF when $M_{bol} < -4$, agrees with the M31 measurements to within the estimated uncertainties, indicating that the bright stellar contents in the bulges of M31 and the Milky-Way are similar.

3.2. Comparisons with Previous Near-Infrared Studies of the M31 Bulge

Rich & Mould (1991) and Rich et al. (1993) obtained deep J and K images of five M31 bulge and inner disk fields, and the ridgelines in the CMDs constructed from these data have $J-K$ colors that are consistent with the CFHT bulge field data. The Rich et al. data also show a tendency for peak brightness to increase towards smaller radii. For example, the brightest giants in Rich et al. (1993) Field 1, located 2.1 arcmin from the center of M31, have $K = 14.5$, while the brightest stars in their Field 3, located 3.9 arcmin from the nucleus, have $K = 15$; the main body of the giant branch in their Field 3 starts at $K = 15.5$, which is in rough agreement with what is seen in Figure 3.

The CFHT bulge field and Rich et al. (1993) Field 1 have similar projected distances from the center of M31, and the peak brightnesses measured from these data differ by roughly 1 magnitude in K, in the sense that the peak brightness infered from the Rich et al. data is brighter. The 0.35 arcsec FWHM angular resolution of the CFHT data is much better than the Rich et al. (1993) data, which have FWHM in the range 1 – 1.2 arcsec, and this can have a major impact on the measured peak brightness; indeed, Rich et al. (1993) suggest that the peak brightness in their Field 1 may be affected by crowding. To confirm this, the CFHT data were convolved with a Gaussian to simulate 1 arcsec seeing. DAOPHOT and ALLSTAR were then used to measure stellar brightnesses in the resulting smoothed image, and the $(K, J-K)$ CMDs of the raw and smoothed datasets are compared in Figure 5. The peak stellar brightness in the smoothed dataset is markedly brighter than in the unsmoothed data, confirming the suggestion made by Rich et al. (1993) that the

brightest stars in their Field 1 are blends.

Stephens et al. (2001b) investigated the stellar content of fields surrounding the globular clusters G174 and G177, which have projected distances from the center of M31 that are comparable to the CFHT bulge field. These data reveal unexpected field-to-field differences in stellar density, as the density of stars is greatest near G177, even though G174 is significantly closer to the center of M31. The brightest field stars near G174 and G177 have $J - K$ colors between 1 and 2, in broad agreement with what is seen in Figure 3. However, the brightest stars have $M_K = -8.4$, which is roughly 0.3 mag fainter than measured from the CFHT data.

The angular resolution of the CFHT data is almost a factor of two worse than the NICMOS data, and so the possibility that the difference in peak brightness is due to crowding is an obvious avenue for investigation. In an effort to determine if the difference in peak stellar brightness between the NICMOS and CFHT data is due to image quality, synthetic H and K datasets with stellar densities comparable to that in the G177 field were created using routines in the IRAF ARTDATA package; the G177 field was selected for detailed modelling because it has a stellar density that is similar to the CFHT bulge field.

Synthetic H and K datasets with FWHM = 0.19 arcsec and FWHM = 0.35 arcsec were constructed. An AGB sequence peaking at K = 16 and with a power-law exponent -0.3, which is comparable to that seen in the Galactic bulge (e.g. Davidge 2000b), was created. The density of AGB stars was fixed according to the number of objects observed in the top K magnitude interval in the G177 field. An RGB component was also included, with the peak brightness and relative number density of these stars, measured with respect to the AGB, based on those seen in the outer regions of M32 by Davidge (2000a). The AGB and RGB sequences were terminated at $K = 20$, which is 2.5 mag below the approximate faint limit of the CFHT data; over 10000 stars were thus added to each frame. Finally, all of the stars were assigned an $H - K$ color of 0.0, and the PSF was assumed to be a gaussian.

The simulations are idealised in that they do not include the effects of, among other factors, (1) residuals in the flat-field and thermal background patterns, (2) anisoplanicity, and (3) intrinsic star-to-star color variations. Hence, the observed scatter in the $(K, H - K)$ CMDs obtained from the simulated images, which are shown in Figure 6, is significantly smaller than in the actual observations. Nevertheless, these simulations indicate that (1) crowding produces a modest population of spuriously bright sources in the G177 field even when FWHM = 0.19 arcsec, and (2) the number of such sources increases only by a factor of $1.5 - 2$ when the FWHM = 0.35 arcsec.

The most conspicuous artifacts of crowding in Figure 6 are sources that are 0.4 -

0.5 magnitude brighter than the AGB-tip; while two such objects are seen in the 0.19 arcsec dataset, three are present in the 0.35 arcsec data. There is also a population of objects 0.05 – 0.15 magnitude above the AGB-tip in both datasets. Aside from the easily identifiable population of blends, in both cases the AGB-tip at $K = 16$ is well-defined, although with 0.35 arcsec FWHM images the peak brightness might be infered to be 0.1 mag brighter than when the FWHM = 0.19 arcsec. Thus, crowding will cause the peak stellar brightness measured from the CFHT data to be at most 0.1 mag brighter than that measured from the NICMOS data.

These simulations suggest that the difference in peak brightness with respect to the Stephens et al. (20001b) data is not due entirely to crowding. Perhaps the photometric calibrations of the two datasets differ at the 0.1 – 0.2 magnitude level, and this speculation will require an independent set of observations to be confirmed. For the time being, it is worth noting that the peak brightness and number density of the brightest stars measured in the CFHT bulge field are consistent with the central M31 field (§4). Not only does this consistency lend confidence to the photometric calibration of the CFHT data, which were recorded over two observing runs, but it also reinforces the nature of the brightest objects as individual stars, and not artifacts of crowding. The excellent agreement between the CFHT bulge field and BW LFs in Figure 4 is also reassuring.

3.3. Comparison with M32

The RGB-tip brightnesses of M31 and M32 agree to within 0.2 mag in I (Davidge & Jones 1992, Davidge 1993), suggesting that these galaxies are roughly equidistant, and this simplifies efforts to compare the bright stellar contents of these systems. Such a comparison is of interest since there are indications that M31 and M32 interacted in the past (Byrd 1975, 1978; Sofue & Kato 1981), raising the possiblity of co-ordinated major star-forming episodes. Moreover, Luppino & Tonry (1993) studied surface brightness flucuations in both galaxies at infrared wavelengths, and found significant differences in the characteristic flucuation brightness. Differences in the bright stellar contents of these systems might then be expected.

The K LFs of the M32 outer and M31 bulge fields are compared in Figure 7, where the M32 LF has been scaled to match the stellar density in the M31 bulge field using the r-band surface brightnesses measured by Kent (1987). It is evident that the M31 and M32 LFs differ by roughly a factor of three between $K = 16.5$ and $K = 17.5$, and the remainder of this section is devoted to exploring possible causes of this difference.

The stellar density in the M31 bulge field is significantly higher than in the M32 outer field ($\mu_r = 18.8$ for the M31 bulge field versus $\mu_r = 22.5$ for the outer M32 field), raising the possibility that the difference in Figure 7 could be due to crowding; indeed, the relative differences between the M31 bulge and M32 LFs in Figure 7 increases towards fainter brightnesses, as expected if crowding were a factor. However, simple arguements suggest that crowding does not significantly affect star counts in the M31 bulge field at the brightnesses where differences with respect to M32 are seen. If it is assumed that the M31 bulge and M32 have similar stellar contents, then the scaled M32 LF predicts that there will be 1850 stars with $K = 18 \pm 0.25$ in the M31 bulge field, most of which are evolving near the RGB-tip. If each resolution element has a diameter comparable to the FWHM of the PSF, then there will be roughly 200 blends among these sources in the bulge field, and these blended objects will appear as sources with $K \sim 17.5$; after correcting for incompleteness, this is roughly 10% of the objects detected with $K = 17.5 \pm 0.25$ in the bulge field. A similar calculation shows that an even smaller fraction of the sources at $K \sim 17$ are blends. Thus, blending can not produce the factor of three difference between the M31 and M32 datasets.

The comparison in Figure 7 assumes that M31 and M32 are equidistant. However, the observed differences could be produced if the bright stellar contents of these systems are in fact similar but their distance moduli differ by ~ 0.5 dex, in the sense that M32 is more distant. This is not consistent with the RGB-tip brightnesses of these systems. Davidge (1993) finds that the RGB-tip occurs at $I = 20.7$ in M31. While the RGB-tip is not well-defined in M32, it appears to be at least as bright as in M31, and may even be 0.2 mag brighter (Freedman 1989; Davidge & Jones 1992). If M32 is closer than M31 then the actual differences between the bright stellar contents of the two fields will be even greater than indicated in Figure 7.

The comparison in Figure 7 assumes that the $r - K$ colors of the two fields are similar, and this may not be the case. Frogel et al. (1978) and Persson et al. (1980) published wide aperture ($d > 100$ arcsec) $V - K$ colors of M32 and M31, and these data indicate that the $V - K$ color of M32 is $\sim 0.1 - 0.2$ mag bluer than M31. However, such a difference in color can account for only part of the differences in Figure 7.

In summary, crowding and differences in broad-band colors may account for roughly one third of the difference seen in Figure 7; thus, it appears that the AGB LFs of the M31 bulge and M32 are intrinsically different, in that the relative density of AGB stars in M32 with K between 16.5 and 17.5 is lower than in the M31 bulge. In §4 this comparison is extended to data sampling the central regions of both galaxies.

4. THE CENTRAL FIELD

The stellar density climbs rapidly with decreasing radius near the center of M31, with the result that the degree of crowding, which affects the completeness fraction and photometric errors, varies significantly across the central field. Given the steep density gradient, and also recognizing that changes in stellar content could occur over small angular scales near the galaxy center, it was decided to investigate the stellar content in 4 annuli centerered on the nuclear source P2.

It is unlikely that individual stars are resolved with the current data within a few arcsec of the galaxy nucleus. Using near-infrared images of the Galactic Center that were processed to simulate the appearance of this field if viewed at the distance of M31, Davidge et al. (1997) concluded that any objects detected at 2μm within ~ 2 arcsec of the M31 nucleus, which corresponds to the point at which the kinematic and photometric properties of M31 depart from the trends defined at larger radii (Kormendy & Bender 1999), are likely blends of fainter stars, even when working at angular resolutions near the diffraction limit of a 4 metre telescope. However, as demonstrated below, the effects of blending decrease significantly at distances in excess of 2 arcsec of the nucleus; although blending still occurs at these radii, the effects can at least be monitored with simulations. Working outwards from 2 arcsec, the radial extent of each annulus was defined such that the number of stars between $K = 15.25$ and $K = 16.25$ was more-or-less evenly distributed between the annuli. The inner and outer radii of each annulus, with distances measured from the nuclear source P2, are listed in Table 1.

The $(K, H - K)$ CMDs of each annulus are shown in Figure 8; the $(K, J - K)$ CMDs are not considered here because of the relatively poor angular resolution of the J data, and the resulting complications introduced by blending. The ridgelines of the AGB sequences in all 4 annuli and the bulge field are in excellent agreement. The brightest stars have $H - K = 0.4$, which is consistent with the colors of late M giants in BW (e.g. Table 3 of Frogel & Whitford 1987). The scatter predicted by the artificial star experiments matches the width of the giant sequences in all 4 annuli, indicating that random uncertainties in the photometric measurements, rather than an intrinsic dispersion in stellar properties, dominate the width of the CMDs.

The CMDs of annuli 3 and 4 and the bulge field are very similar: in each case the main stellar sequence terminates near $K = 15.7 - 15.6$, and there is a spray of stars $\sim 0.1 - 0.2$ mag above this point. It is also worth noting that the bright portions of the CMDs of annuli 3 and 4 are similar to the simulations shown in Figure 6. As for annuli 1 and 2, the AGB sequences are continuous to brighter values than in annuli 3 and 4, peaking near $K = 15.5$ in annulus 2, and $K = 15.3$ in annulus 1.

An increase in peak stellar brightness towards progressively more crowded environments is a classic signature of blending. The stellar density in annulus 1 is roughly twice that in annulus 4, and so pairs of sub-regions in annulus 4 were summed to create simulated fields with densities comparable to that in annulus 1. Two pairs of 200×200 pixel regions in annulus 4 were summed, and the brightnesses of stars in the summed images were then measured using DAOPHOT. The CMDs of sources in the sub-regions prior to, and after, summing are compared in Figure 9. The CMDs of sources in the summed fields and in annulus 1 are very similar, lending confidence to the simulations. It is evident from Figure 9 that a factor of two increase in stellar density has a marked influence on the bright portions of the CMD at these densities, in that the peak brightness is elevated by 0.1 - 0.2 mag in K. Hence, the apparent trend of increasing peak giant branch brightness with decreasing radius in Figure 8 is the result of blending; this is contrary to the conclusion reached by Davidge et al. (1997), who did not have the benefit of data obtained at larger radii to gauge the effects of blending.

The number density of infrared-bright stars scales with $r-$band surface brightness throughout the inner bulge of M31. This is demonstrated in Figure 10, where the K LFs of annuli 1 – 4 are compared with the K LF of the bulge field, after the latter was scaled to match the mean r-band surface brightness in each annulus based on the Kent (1987) light profile; the LFs in this figure have been corrected for incompleteness, and are restricted to the bright end where sample incompleteness does not exceed 70%. The LFs of annuli 3 and 4 are well matched by the LF of the bulge field at all brightnesses. There is an excess number of sources with $K = 15.5$ in annuli 1 and 2 when compared with the scaled bulge field population, and the simulations discussed in the previous paragraph suggest that this is the result of crowding, although the agreement at $K = 16$ and $K = 16.5$ is excellent. It thus appears that the radial distribution of the brightest stars at infrared wavelengths in the M31 bulge tracks the $r-$band light profile of the galaxy, even to within a few arcsec of the nucleus.

Local mass density influences the star-forming history of regions within galaxies (e.g. Bell & de Jong 2000; Martinelli, Matteucci, & Colafrancesco 1998; Franx & Illingworth 1990); galaxy-to-galaxy comparisons between areas having similar densities will remove this dependence, and thereby provide a better means of searching for inherent differences in stellar content. Davidge et al. (2000) obtained H and K observations with 0.12 arcsec FWHM resolution of the central regions of M32, and the mean surface brightness in Region 3 of the Davidge et al. (2000) study is comparable to that in annuli 2 and 3 of the M31 central field. The K LFs of M32 Region 3 and the sum of annuli 2 and 3 are compared in Figure 11. The agreement between the M31 and M32 LFs is much better than in Figure 7, although the M31 and M32 LFs differ by a significant amount at $K = 16.5$, and the M31

LF falls consistently above that of M32 when $K > 16.5$, as would be expected from Figure 7. Nevertheless, the improved agreement between the M31 and M32 LFs at the faint end suggests that crowding may affect significantly the comparison in Figure 7 at $K = 17.5$. We conclude that while the comparisons between the LFs of the M31 bulge and M32 in Figures 7 and 11 are *suggestive* of a difference in bright stellar content, in the sense that the number density of moderately bright AGB stars is lower in M32 than in the bulge of M31, the results are far from conclusive, and should be confirmed with data having higher angular resolutions to reduce the effects of crowding.

5. DISCUSSION & SUMMARY

Images with angular resolutions approaching the diffraction limit of the 3.6 metre CFHT have been used to investigate the infrared-bright stellar content of the inner bulge of M31. The number density of the brightest stars in K scales with $r-$band surface brightness in the central few arcmin of the galaxy. This indicates that (1) these objects are well mixed throughout the main body of the inner bulge, and thus belong to a population that formed in a highly coherent manner, and (2) the brightest stars do not belong to the disk (see also Rich et al. 1993), since the light profile of the galaxy is dominated by the bulge at small radii. Previous investigations of the stellar content of the M31 bulge are reviewed in §5.1, and it is concluded that the bulge is dominated by a population of old stars. Building on this result, it is argued in §5.2 that the infrared-bright AGB stars are old objects, and this interpretation is consistent with the spatial distribution of these stars.

5.1. The Stellar Content of the M31 Bulge

In recent years there has been a growing realization that the bulges of spiral galaxies do not evolve in isolation; rather, the diversity evident in the central morphological (e.g. Carollo, Stiavelli, & Mack 1998) and overall structural (Carollo 1999) characteristics of spiral galaxies suggests that bulges are influenced by external environmental factors. The disk is an obvious source of star-forming material, and evidence that the evolution of the bulge and surrounding disk are coupled comes from the correlated ages (Peletier & Balcells 1996) and structural characteristics (Andredakis, Peletier, & Balcells 1995) of these systems. Bar instabilities (e.g. Friedli & Benz 1993, 1995), galaxy-galaxy interactions (e.g. Barnes & Hernquist 1992, Mihos & Hernquist 1996), and dynamical friction (Noguchi 1999, 2000) are three mechanisms by which gas and stars from the disk can be channeled into the central regions of bulges.

Is there evidence for a mixture of stellar ages in the bulge of M31? Imaging surveys indicate that the bulge of M31 does not contain young stars. The brightest members of a very young population have blue colors, and Brown et al. (1998) argue that the majority of resolved sources detected in the UV near the nucleus of M31 are evolving on the extended HB rather than the main sequence. Based on the faint limit of their data, Brown et al. (1998) conclude that the youngest UV-bright stars in the M31 bulge have an age in excess of 250 Myr.

Spectroscopic studies at visible wavelengths suggest that stars spanning a range of ages are present within a few arcsec of the center of M31. Both Davidge (1997) and Sil'Chenko et al. (1998) find evidence for an age gradient near the center of the galaxy, indicating that any intermediate age component in the central regions of M31 is centrally concentrated, and has a spatial distribution that differs from that of the main body of the bulge. The intermediate-age population does not dominate the innermost regions of the M31 bulge. Bica et al. (1990) used evolutionary synthesis techniques to investigate the integrated visible spectrum of the central few arcsec of M31 and found that, even near the galaxy center, the bulge is dominated by an old population. In addition to an intermediate-age component that contributes a modest fraction of the integrated light at visible wavelengths, Bica et al. (1990) also found evidence of stars as young as 10 Myr, although the presence of such a population is not supported by UV imaging data.

There is other evidence indicating that the bulges of type Sbc and earlier spirals are dominated by old populations. In the case of the Milky-Way, Feltzing & Gilmore (2000) examined HST images of Galactic bulge fields, and concluded that disk contamination is responsible for the relatively bright blue stars that have heretofore been associated with an intermediate-age population. Once disk contamination is taken into account, Feltzing & Gilmore (2000) conclude that the main body of the bulge has an old age, in agreement with the bulge (Minniti 1995) globular cluster system (e.g. Ortolani et al. 1995; Fullton et al. 1995). Finally, the colors of nearby (Peletier et al. 1999) and distant (Abraham et al. 1999) spiral galaxies indicate that the bulges of these systems contain a significant component that formed early-on.

The central regions of the Galaxy contain stars spanning a range of ages. There are compact star clusters near the GC (Cotera et al. 1996, Figer et al. 1999) with ages of a few Myr, indicating that star formation can (and does) occur in the innermost regions of the Galaxy. While it can be argued that these clusters do not belong to the bulge, they have short dynamical timescales (e.g. Figer et al. 1999), and hence quickly evaporate and contribute to the field population in the innermost regions of the galaxy. We speculate that the centrally concentrated intermediate age population in M31, which has a spatial

distribution that is different from the underlying bulge, may be an artifact of an earlier star-forming event similar to that recently experienced by the GC.

In summary, while signatures of an intermediate age population may be present in integrated spectra of the center of M31, this population is centrally concentrated, and is not a major constituent of the bulge, which is dominated by old stars. A dominant old population is consistent with the non-solar [Mg/Fe] ratio of stars in the M31 bulge found by Davidge (1997), which is suggestive of a rapid initial chemical enrichment by SN II, as expected if the M31 bulge experienced a rapid (t $<$ 1 Gyr) collapse during early epochs. The bulge of M31 has apparently not been subject to the external sources of star forming material or intermediate age and younger stars discussed in the opening paragraph of this section.

5.2. The Nature of the Brightest AGB stars in the M31 Bulge

The brightest AGB stars in the M31 bulge follow the integrated light profile of the galaxy and have a peak brightness that does not change measureably with radius. The brightest stars at infrared wavelengths are therefore well mixed throughout the inner bulge; these stars can not belong to an intermediate-age population, which the spectroscopic data suggests is more centrally concentrated than the main body of the bulge (Davidge 1997). Thus, the infrared-bright AGB stars likely belong to the old population that dominates the bulge of M31.

The brightest stars in the compact elliptical galaxy M32 share common characteristics with their counterparts in the bulge of M31 in that they (1) have a similar peak brightness, and (2) are uniformly mixed throughout the galaxy (Davidge 2000a; Davidge et al. 2000). The brightness of the AGB-tip is more sensitive to metallicity than age in stellar systems with ages exceeding a few Gyr. If the MDF of the M31 bulge field is similar to that in BW, then the majority of stars in this field will have metallicities close to solar, and there will also be a population of super metal-rich objects (McWilliam & Rich 1994). AGB-tip stars in old moderately metal-rich globular clusters have brightnesses approaching those of the brightest stars in M32 and the M31 bulge; for example, stars as bright as $M_K = -8.5$ are present in the [Fe/H] = -0.34 (Harris 1996) globular cluster NGC 6553 (Guarnieri, Renzini, & Ortolani 1997), and even brighter AGB-tip stars should occur in a population that is more metal-rich. We thus suggest that the brightest AGB stars in M32 and the Galactic and M31 bulges are very metal-rich: these stars are bright not because of their age, but because of their chemical composition. Given that the mean metallicity of M32 is lower than that in the bulge of M31 (Bica et al. 1990), then the number density of bright AGB

stars at a given surface brightness should be lower in the former than in the latter, and this is consistent with the comparisons between the K LFs of these systems, which are discussed in §3 and 4, although clearly the differences seen between the bright stellar contents of M32 and the M31 bulge need to be confirmed with data having higher angular resolutions.

The brightest stars in M32 and the M31 bulge have similar peak brightnesses; given that the brightness of the AGB-tip depends more on metallicity than age among old populations, then it might be anticipated that the brightest stars in these systems have similar metallicities, and this prediction can be tested spectroscopically. The targets are relatively bright, with $K = 15.5 - 16.0$; hence, the observational challenge is not one of obtaining a large S/N ratio, but of resolving individual stars in crowded environments. AO-fed integral-field spectrographs will be essential for obtaining uncontaminated spectra of these stars.

It is a pleasure to thank the anonymous referee for providing a comprehensive report containing suggestions that greatly improved the paper.

Annulus #	Radii (arcsec)
1	2.0 – 7.8
2	7.8 – 11.9
3	11.9 – 15.3
4	15.3 – 24.0

Table 1: Radial Intervals for Annuli in the Central Field

REFERENCES

Abraham, R. G., Ellis, R. S., Fabian, A. C., Tanvir, N. R., & Glazebrook, K., 1999, MNRAS, 303, 641

Andredakis, Y., Peletier, R. F., & Balcells, M. 1995, MNRAS, 275, 874

Barnes, J. E., & Hernquist, L. E. 1992, ARA&A, 30 705

Bell, E. F., & de Jong, R. S. 2000, MNRAS, 312, 497

Bica, E., Alloin, D., & Schmidt, A. A. 1990, A&A, 228, 23

Bohlin, R. C., Cornett, R. H., Hill, J. K., Hill, R. S., O'Connell, R. W., & Stecher, T. P. 1985, ApJ, 298, 37

Brown, T. M., Ferguson, H. C., Stanford, S. A., & Deharveng, J-M 1998, ApJ, 504, 113

Byrd, G. G. 1976, ApJ, 208, 688

Byrd, G. G. 1978, ApJ, 226, 70

Carollo, C. M. 1999, ApJ, 523, 566

Carollo, C. M., Stiavelli, M., & Mack, J. 1998, AJ, 116, 68

Casali, M., & Hawarden, T. 1992, JCMT-UKIRT Newsletter, 4, 33

Cotera, A. S., Erickson, E. F., Colgan, S. W. J., Simpson, J. P., Allen, D. A., & Burton, M. G. 1996, ApJ, 461, 750

Davidge, T. J. 1993, ApJ, 409, 190

Davidge, T. J. 1997, AJ, 113, 985

Davidge, T. J. 2000a, PASP, 112, 1177

Davidge, T. J. 2000b, AJ, 120, 1853

Davidge, T. J. 2001, AJ, 121, 3100

Davidge, T. J., & Courteau, S. 1999, AJ, 117, 1297

Davidge, T. J., & Jones, J. H. 1992, AJ, 104, 1365

Davidge, T. J., Le Févre, O., & Clark, C. C. 1991, ApJ, 370, 559

Davidge, T. J., Rigaut, F., Doyon, R., & Crampton, D. 1997, AJ, 113, 2094

Davidge, T. J., Rigaut, F., Chun, M., Brandner, W., Potter, D., Northcott, M., Graves, J. E. 2000, ApJL, 545, L89

Davies, R. L., Frogel, J. A., & Terndrup, D. M. 1991, AJ, 102, 1729

DePoy, D. L., Terndrup, D. M., Frogel, J. A., Atwood, B., & Blum, R. 1993, AJ, 105, 2121

Dressler, A., & Richstone, D. O. 1988, ApJ, 324, 701

Feltzing, S., & Gilmore, G. 2000, A&A, 355, 949

Ferguson, H. C., & Davidsen, A. F. 1993, ApJ, 408, 92

Figer, D. F., Kim, S. S., Morris, M., Serabyn, E., Rich, R. M., & McLean, I. S. 1999, ApJ, 525, 750

Franx, M., & Illingworth, G. 1990, ApJ, 359, L41

Freedman, W. L. 1989, AJ, 98, 1285

Friedli, D., & Benz, W. 1993 A&A, 268, 65

Friedli, D., & Benz, W. 1995 A&A, 609, 649

Frogel, J. A., & Whitford, A. E. 1987, ApJ, 320, 199

Frogel, J. A., Persson, S. E., Aaronson, M., & Matthews, K. 1978, ApJ, 220, 75

Fullton, L. K. et al. 1995, AJ, 110, 652

Guarnieri, M. D., Renzini, A., & Ortolani, S. 1997, ApJ, 477, L21

Harris, W. E. 1996, AJ, 112, 1487

Jablonka, P., Bridges, T. J., Sarajedini, A., Meylan, G., Maeder, A., & Meynet, G. 1999, ApJ, 518, 627

Kent, S. M. 1987, AJ, 94, 306

King et al. 1992, ApJ, 397, L35

Kormendy, J. 1988, ApJ, 325, 128

Kormendy, J., & Bender, R. 1999, ApJ, 522, 772

Lauer et al. 1993, AJ, 106, 1436

Luppino, G. A., & Tonry, J. L. 1993, ApJ, 410, 81

Martinelli, A., Matteucci, F., & Colafrancesco, S. 1998, MNRAS, 298, 42

McWilliam, A., & Rich, R. M. 1994, ApJS, 91, 749

Mihos, J. C., & Hernquist, L. 1996, ApJ, 464, 641

Minniti, D. 1995, AJ, 109, 1663

Noguchi, M. 1999, ApJ, 514, 77

Noguchi, M. 2000, MNRAS, 312, 194

Ortolani, S. et al. 1995, Nature, 377, 701

Peletier, R. F., & Balcells, M. 1996, AJ, 111, 2238

Peletier, R. F., Balcells, M., Davies, R. L., Andredakis, Y., Vazdekis, A., Burkert, A., & Prada, F. 1999, MNRAS, 310, 703

Persson, S. E., Cohen, J. G., Sellgren, K., Mould, J., & Frogel, J. A. 1980, ApJ, 240, 779

Reid, M. 1993, ARAA, 31, 345

Renzini, A. 1998, AJ, 115, 2459

Rich, R. M., & Mighell, K. J. 1995, ApJ, 439, 145

Rich, R. M., & Mould, J. R. 1991, AJ, 101, 1286

Rich, R. M., Mould, J., & Graham, J. R. 1993, AJ, 106, 2252

Rich, R. M., Mould, J., Picard, A., Frogel, J. A., & Davies, R. 1989, ApJ, 341, L51

Rigaut, F. et al. 1998, PASP, 110, 152

Sil'Chenko, O. K., Burenkov, A. N., & Vlasyuk, V. V. 1998, A&A, 337, 349

Sofue, Y., & Kato, T. 1981, PASJ, 33, 449

Stetson, P. B. 1987, PASP, 99, 191

Stetson, P. B., & Harris, W. E. 1988, AJ, 96, 909

Stephens, A. W., Frogel, J. A., Freedman, W., Gallart, C., Jablonka, P., Ortolani, S., Renzini, A., Rich, R. M., & Davies, R. 2001, AJ, 121, 2584

Stephens, A. W., Frogel, J. A., Freedman, W., Gallart, C., Jablonka, P., Ortolani, S., Renzini, A., Rich, R. M., & Davies, R. 2001, AJ, 121, 2597

van den Bergh, S. 2000, The Galaxies of the Local Group, Cambridge Press, 11

This preprint was prepared with the AAS LaTeX macros v4.0.

FIGURE CAPTIONS

Fig. 1.— The final Ks image of the bulge field. North is at the top, and east is to the left. The image covers 34×34 arcsec, and the angular resolution is 0.35 arcsec FWHM. The bright central source is the star GSC 02801–02015, which served as the reference source for AO compensation.

Fig. 2.— The final Ks image of the central M31 field. North is at the top, and east is to the left. The image covers 34×34 arcsec, and the angular resolution is 0.17 arcsec FWHM.

Fig. 3.— The $(K, J-K)$ and $(K, H-K)$ CMDs of the M31 bulge field. The error bars show the uncertainties predicted from the artificial star experiments, which assume a constant PSF for each field. The good agreement between the predicted and observed scatter indicates that anisoplanicity does not contribute significantly to the photometric errors.

Fig. 4.— The bolometric LFs of the M31 bulge field (solid line) and BW (dashed line). The BW LF was constructed from the bolometric magnitudes listed in Table 1 of Frogel & Whitford (1987), but assuming a distance modulus of 14.5. N_{05} is the number of stars per 0.5 mag bin corrected for incompleteness. The error bars in the M31 LF reflect the uncertainties introduced by counting statistics and the completeness corrections, while the error bars for the BW LF include only counting statistics. The BW LF has been scaled to match the number of stars in the M31 LF when $M_{bol} < -4$. Note that the two LFs agree to within the estimated uncertainties, indicating that the bright stellar content of the M31 bulge is similar to that in BW.

Fig. 5.— The $(K, J-K)$ CMD of the M31 bulge field, as observed with 0.35 arcsec FWHM image quality, compared with the CMD of the same field after convolving with a Gaussian to simulate 1 arcsec FWHM image quality. Note the difference in peak stellar brightness.

Fig. 6.— The $(K, H-K)$ CMDs obtained from simulated images of a field with a stellar density identical to that in the Stephens et al. (2001a) G177 field. The simulated datasets have FWHM = 0.19 arcsec, in agreement with the Stephens et al. data, and 0.35 arcsec, which is the angular resolution of the CFHT bulge field data. Additional details of the models can be found in the text. Note that in both cases there is a smattering of blended objects above the AGB-tip, which occurs at $K = 16$; the brightest of these are well separated from the main body of stars in the CMD, and hence are easily identified. The simulations indicate that when FWHM = 0.35 arcsec the brightness of the AGB-tip may be overestimated by at most 0.1 magnitude in K when compared with data having FWHM = 0.19 arcsec.

Fig. 7.— The K LF of the M31 bulge field (solid line), based on sources detected in both H

and K, compared with the K LF of the M32 outer field (dotted line) observed by Davidge (2000a). N_{05} is the number of stars per 0.5 mag interval. The LFs have been corrected for incompleteness using results from artificial star experiments. The M32 LF has been scaled to match the $r-$band surface brightness of the M31 field using the measurements made by Kent (1987). The error bars show the uncertainties due to counting statistics and the completeness corrections. Note the disagreement between the M32 and M31 LFs between $K = 16.5$ and 17.5.

Fig. 8.— The $(K, H-K)$ CMDs of stars at various distances from the center of M31, including the bulge field. The scatter in the data is well matched by the photometric errors predicted by the artificial star experiments.

Fig. 9.— The effects of image blending are investigated in this figure. The left hand panel shows the composite $(K, H-K)$ CMD of four 200 × 200 pixel sub-regions in annulus 4. The middle panel shows the composite $(K, H-K)$ CMD after these sub-regions were paired and summed to simulate the stellar density in annulus 1. These simulations indicate that a factor of two increase in stellar density elevates the peak stellar brightness by 0.1 – 0.2 mag near the nucleus of M31. The CMD constructed from the summed dataset is remarkably similar to the $(K, H-K)$ CMD of annulus 1, which is shown in the right hand panel.

Fig. 10.— The K LFs of the 4 annuli in the central field (solid lines), constructed from stars detected in both H and K, compared with the K LF of the bulge field (dashed line), which has been scaled to match the $r-$band surface brightness in each annulus using the measurements published by Kent (1987). The LFs have been corrected for incompleteness, based on results from artificial star experiments. n_{05} is the number of stars per square arcsec per 0.5 mag, and the error bars show the uncertainties introduced by counting statistics and the completeness corrections. Note the excellent agreement with the bulge field LF at $K = 16$ and $K = 16.5$ for each annulus. The tendency for the number density of sources at $K = 15.5 \pm 0.25$ in the central field to increase towards smaller radii at a rate that is faster than expected from the bulge field data is likely the result of blending.

Fig. 11.— The K LF of annuli 2 and 3 (solid line) compared with the LF of M32 Region 3 from Davidge et al. (2000), which has an $r-$band surface brightness comparable to that of M31 annuli 2 and 3. n_{05} is the number of stars per square arcsec per 0.5 mag interval. The LFs have been corrected for incompleteness based on the results from artificial star experiments. Note that the M31 and M32 LFs differ significantly only when $K = 16.5$, although the M31 LF falls consistently above that of M32 when $K > 16.5$, as expected from Figure 7.

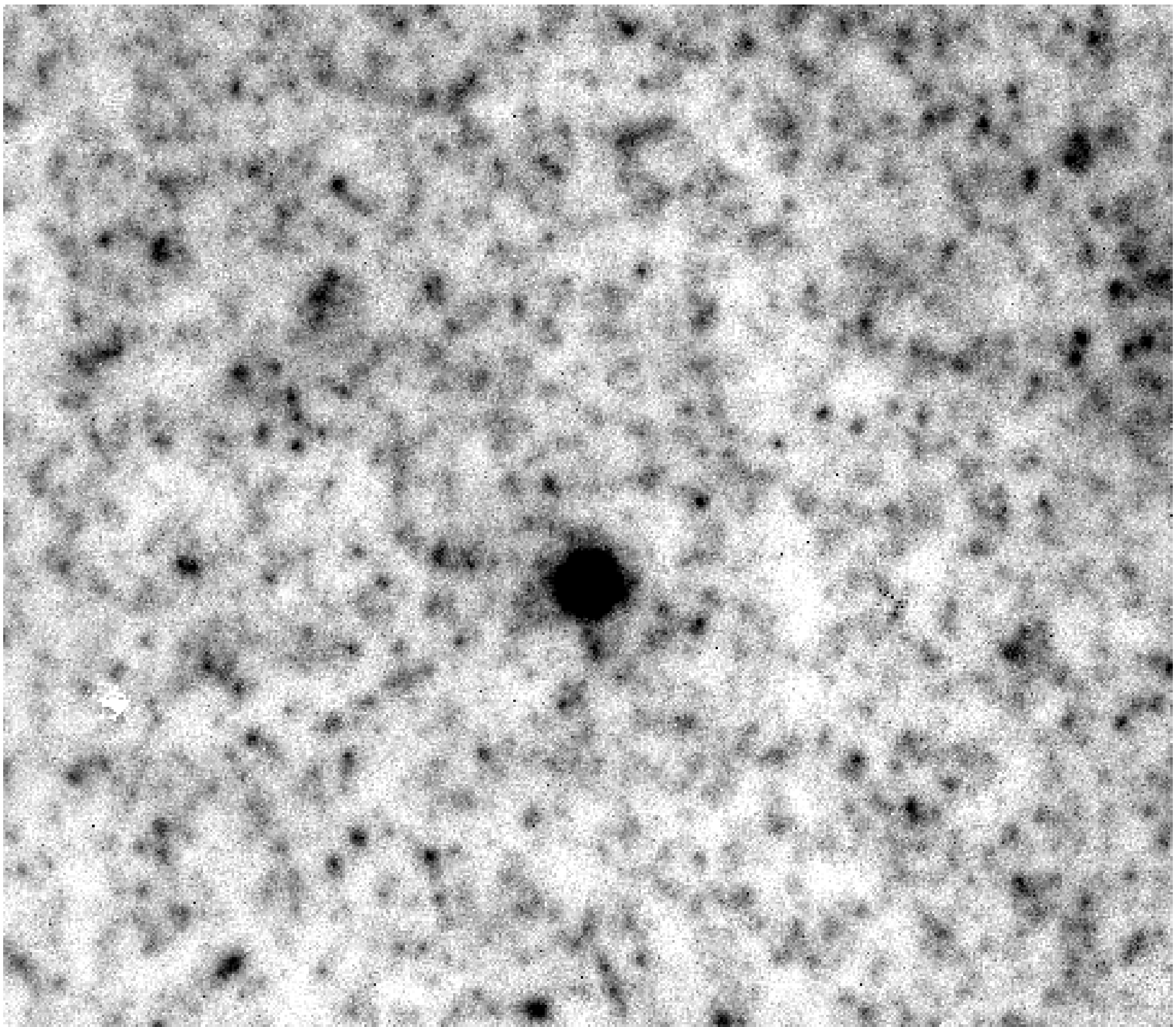

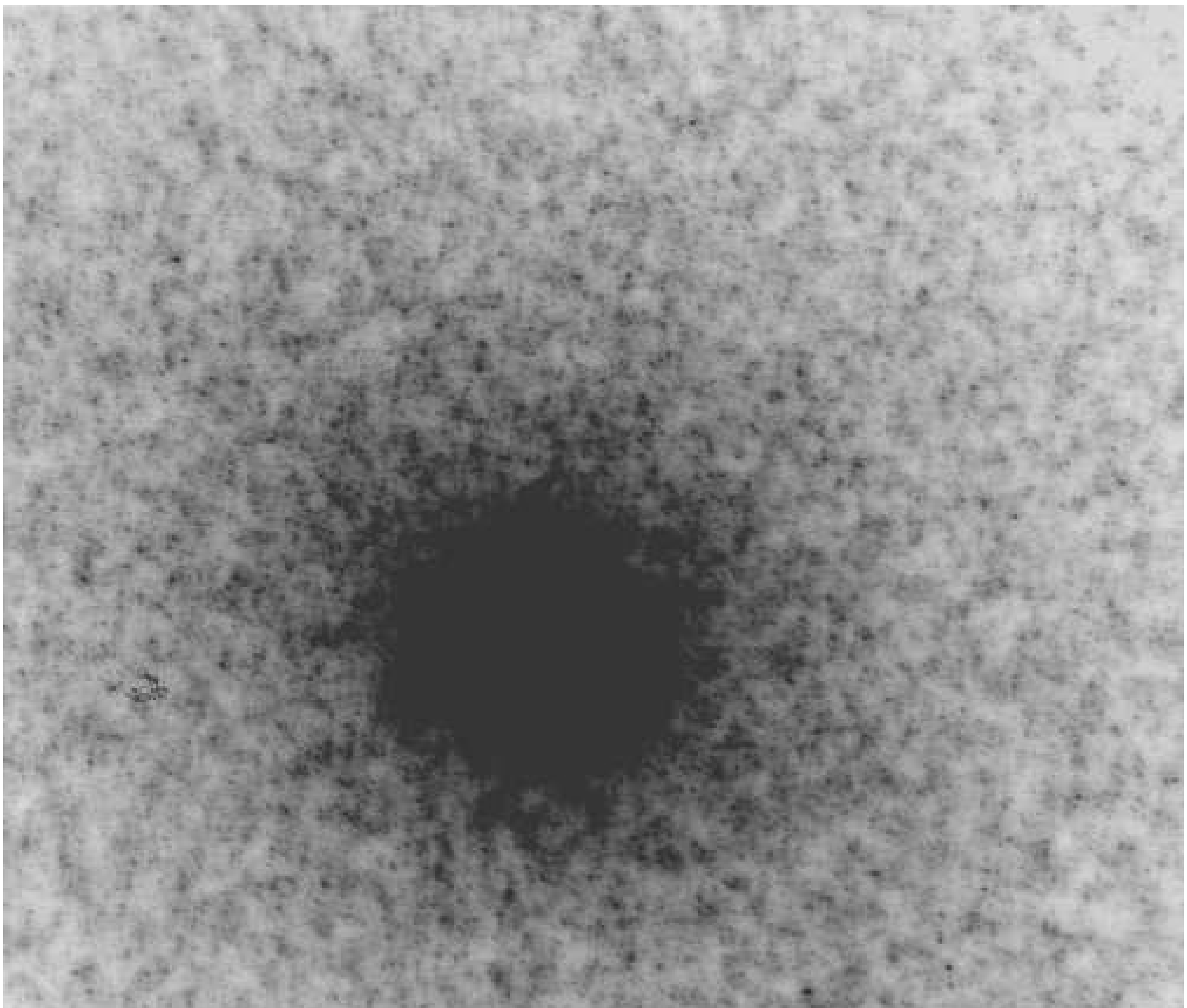

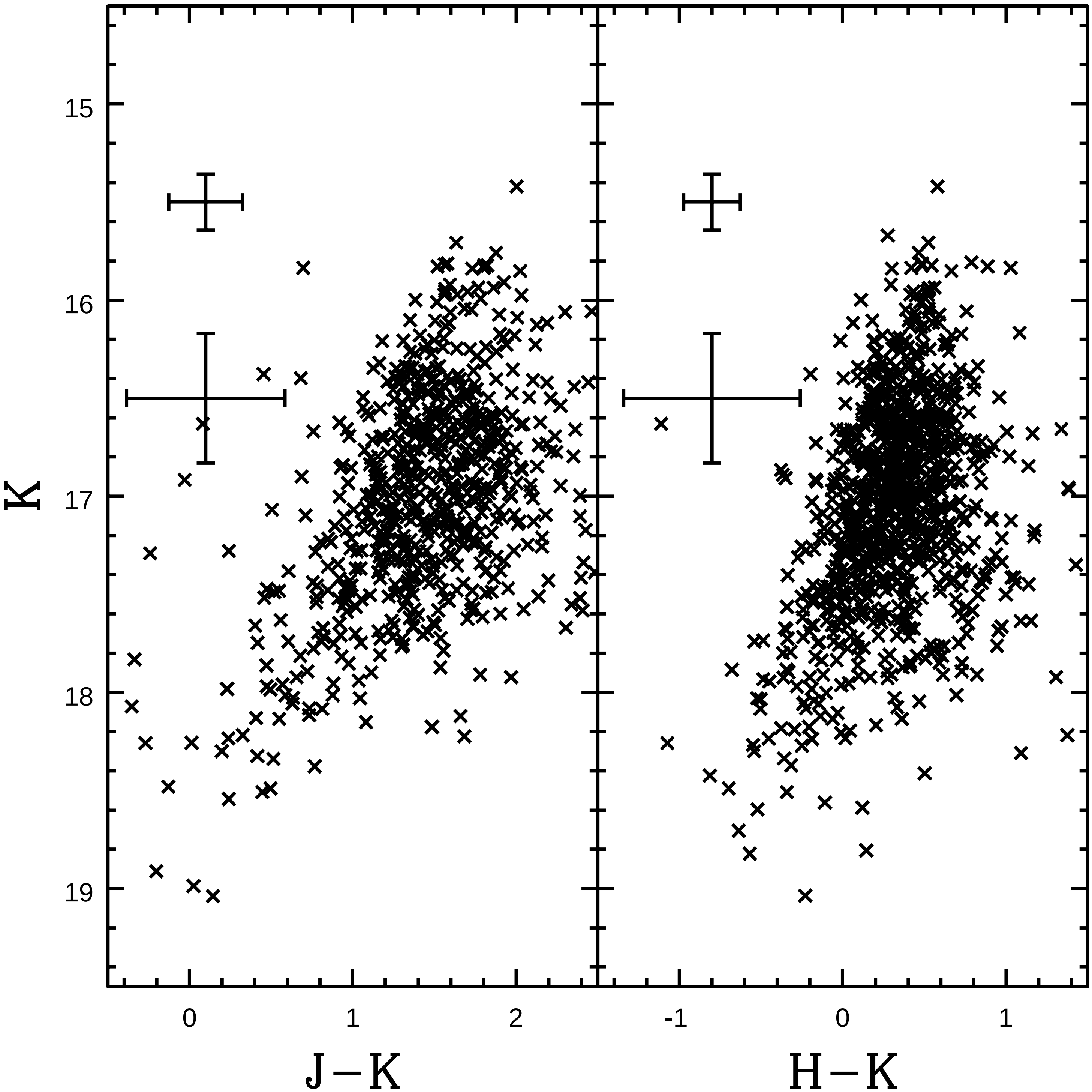

15
16
17
18
19
K
0
1
2
J−K
-1
0
1
H−K

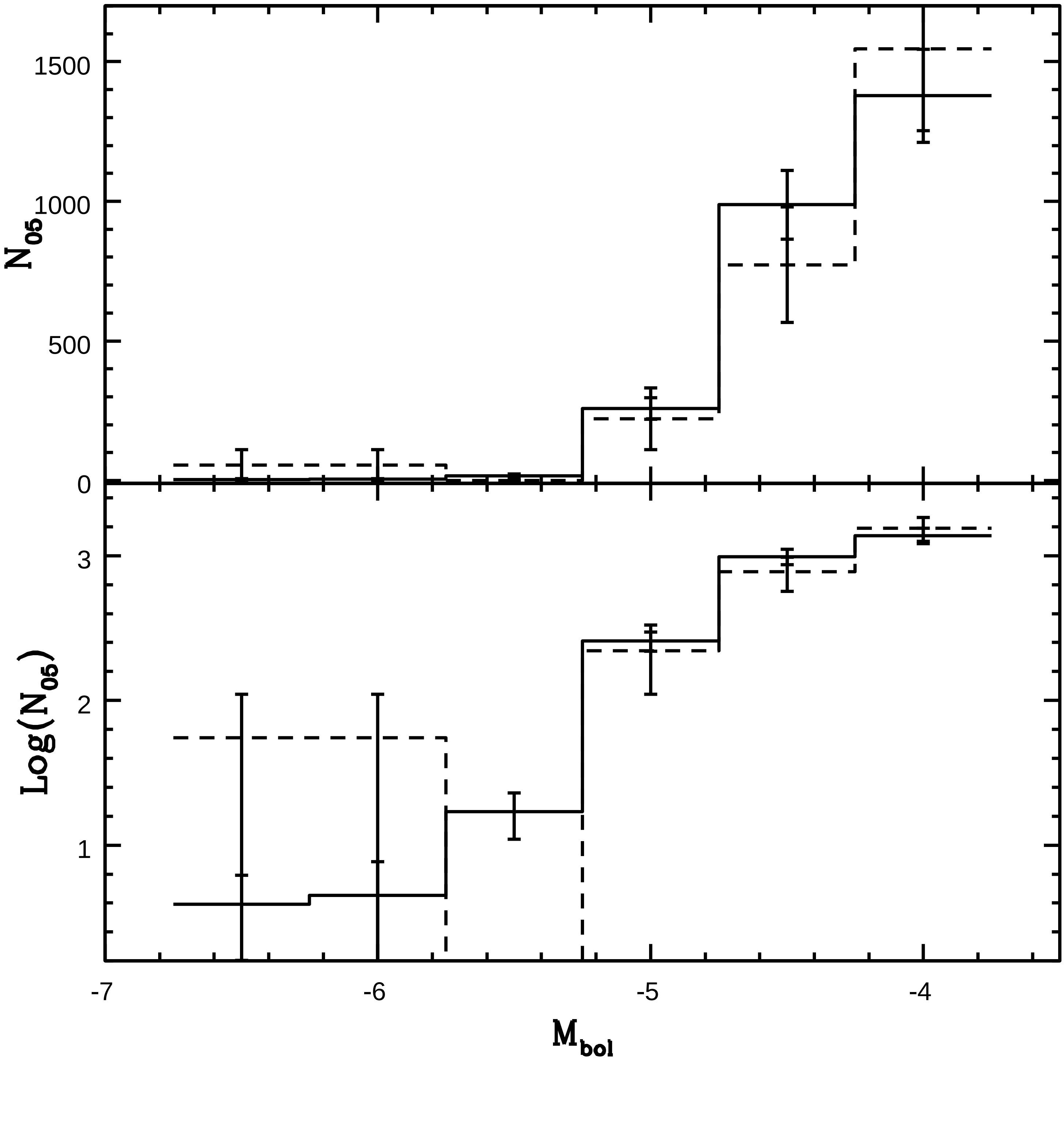

1500
1000
500
0
N_{05}
3
2
1
$Log(N_{05})$
-7
-6
-5
-4
M_{bol}

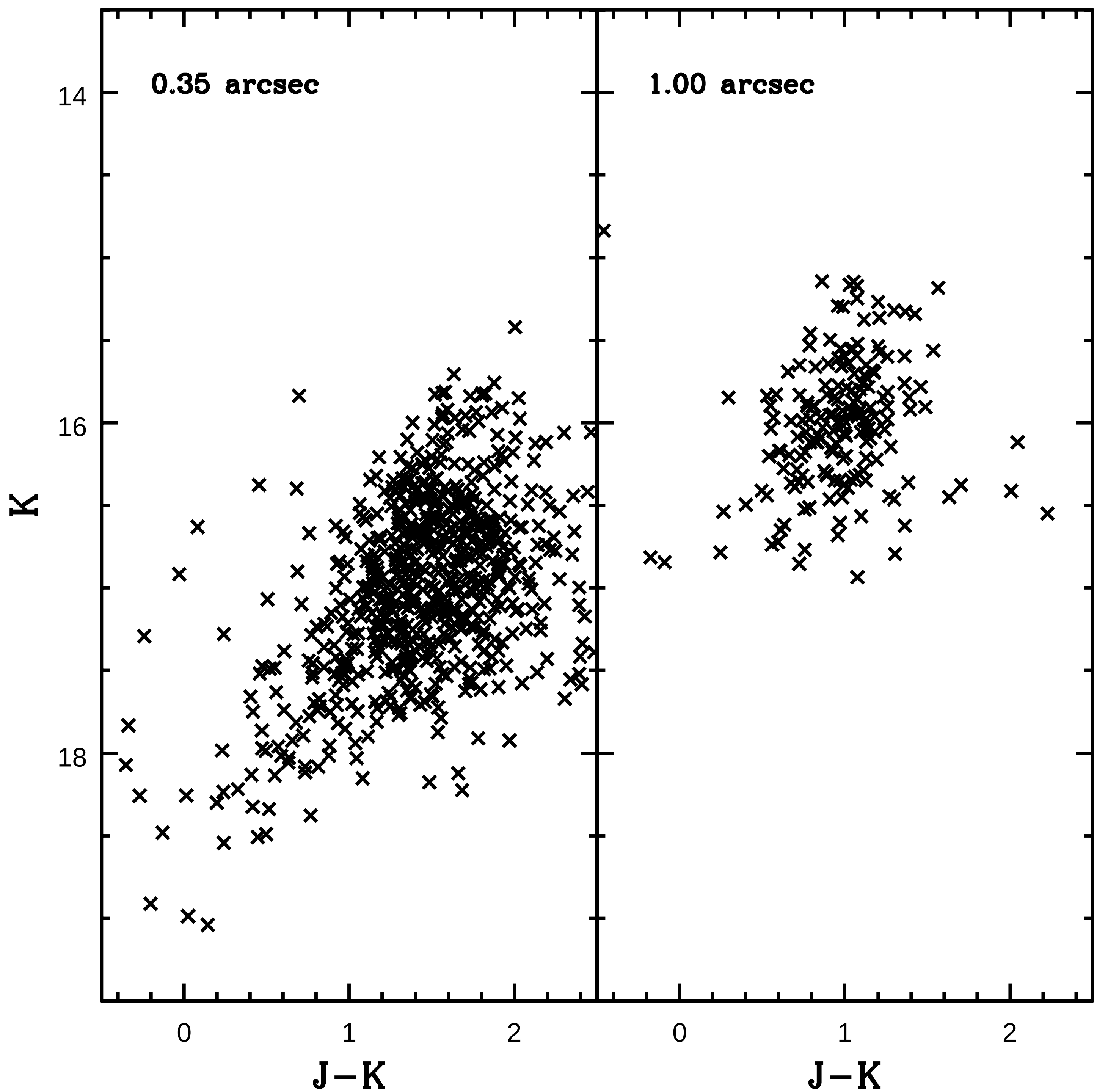

0.35 arcsec
1.00 arcsec
K
14
16
18
J−K
0
1
2
J−K
0
1
2

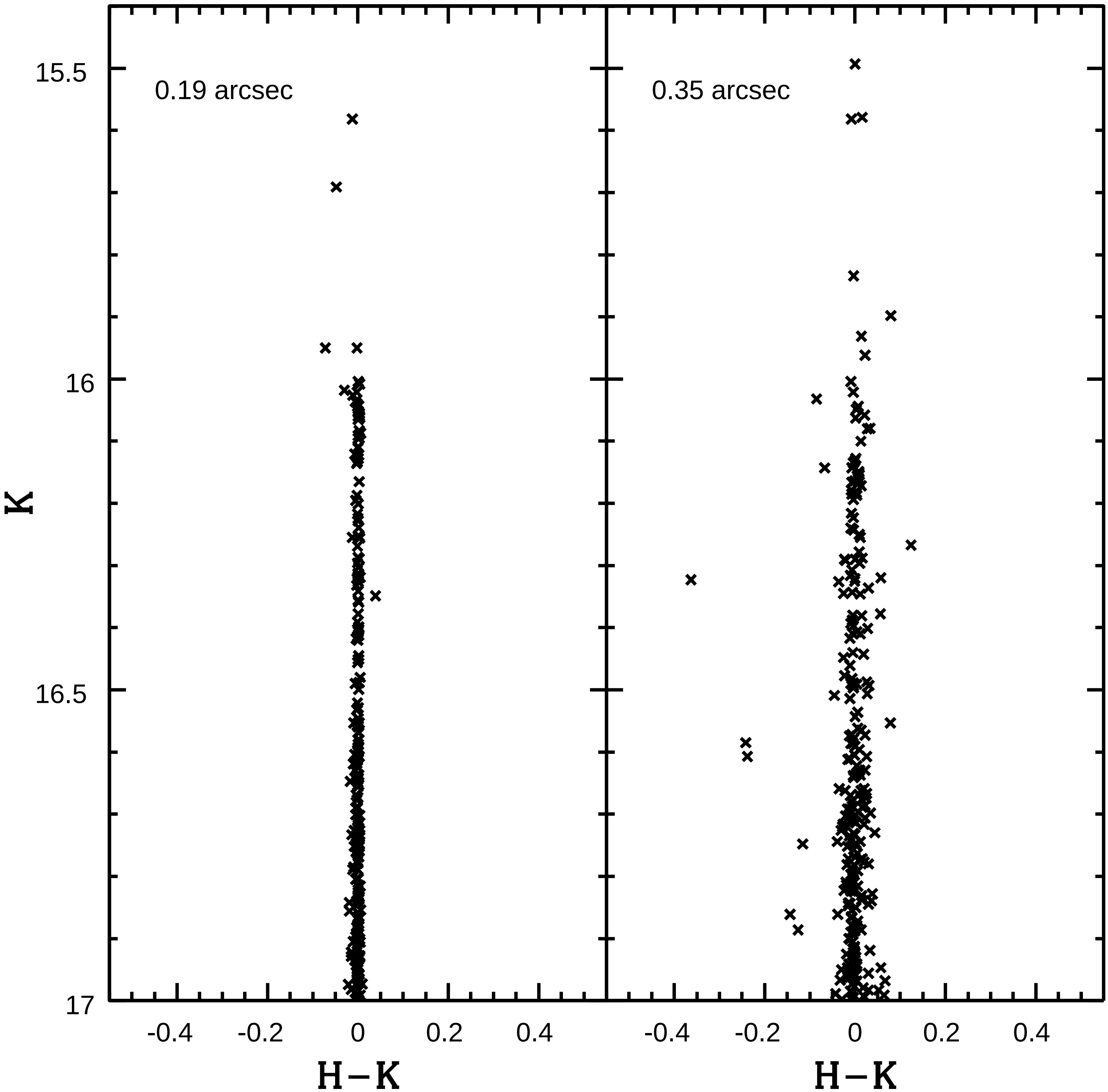
0.19 arcsec
0.35 arcsec
15.5
16
16.5
17
K
-0.4
-0.2
0
0.2
0.4
H−K
-0.4
-0.2
0
0.2
0.4
H−K

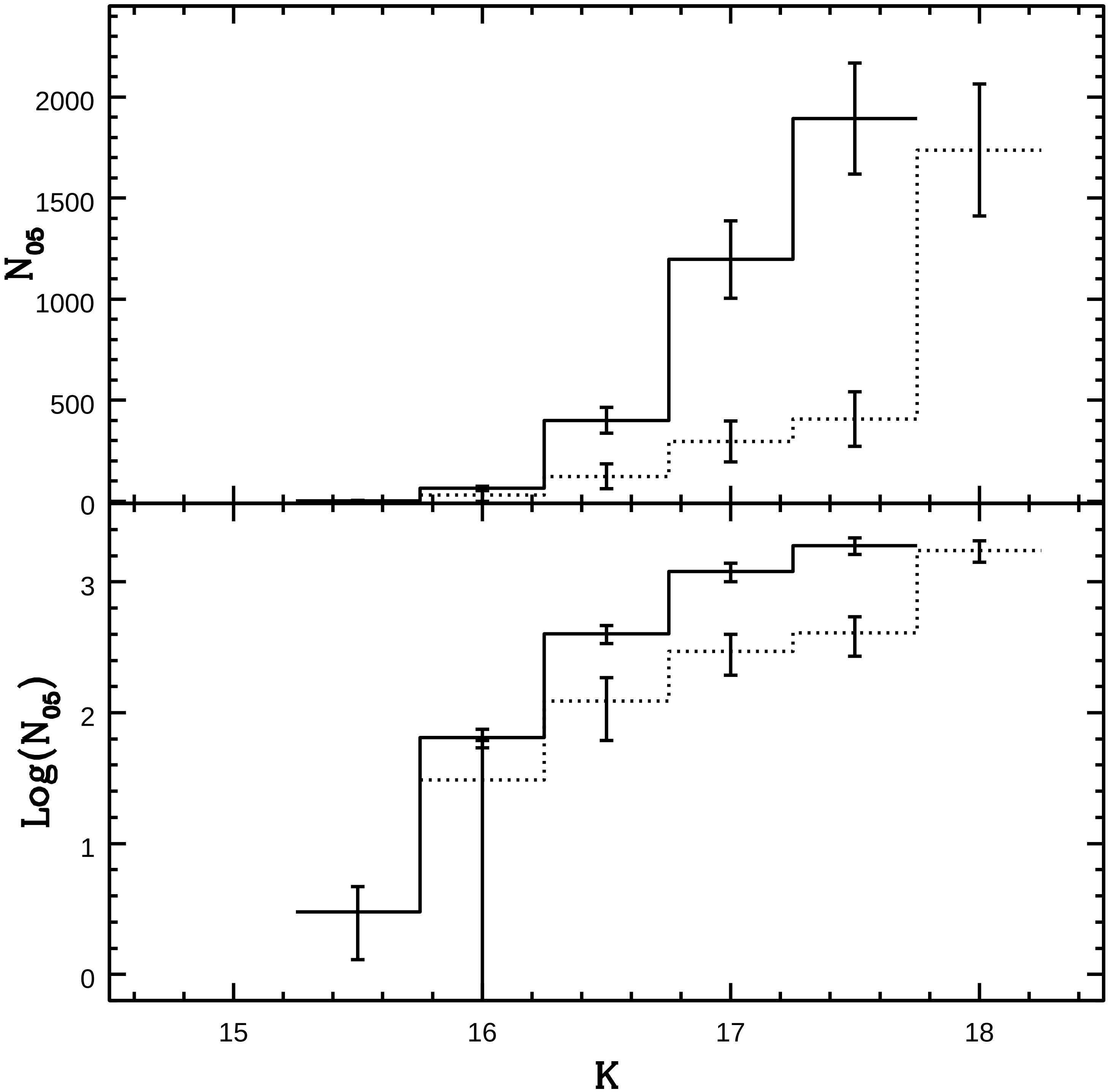

2000
1500
1000
500
0
N_{05}
3
2
1
0
$Log(N_{05})$
15
16
17
18
K

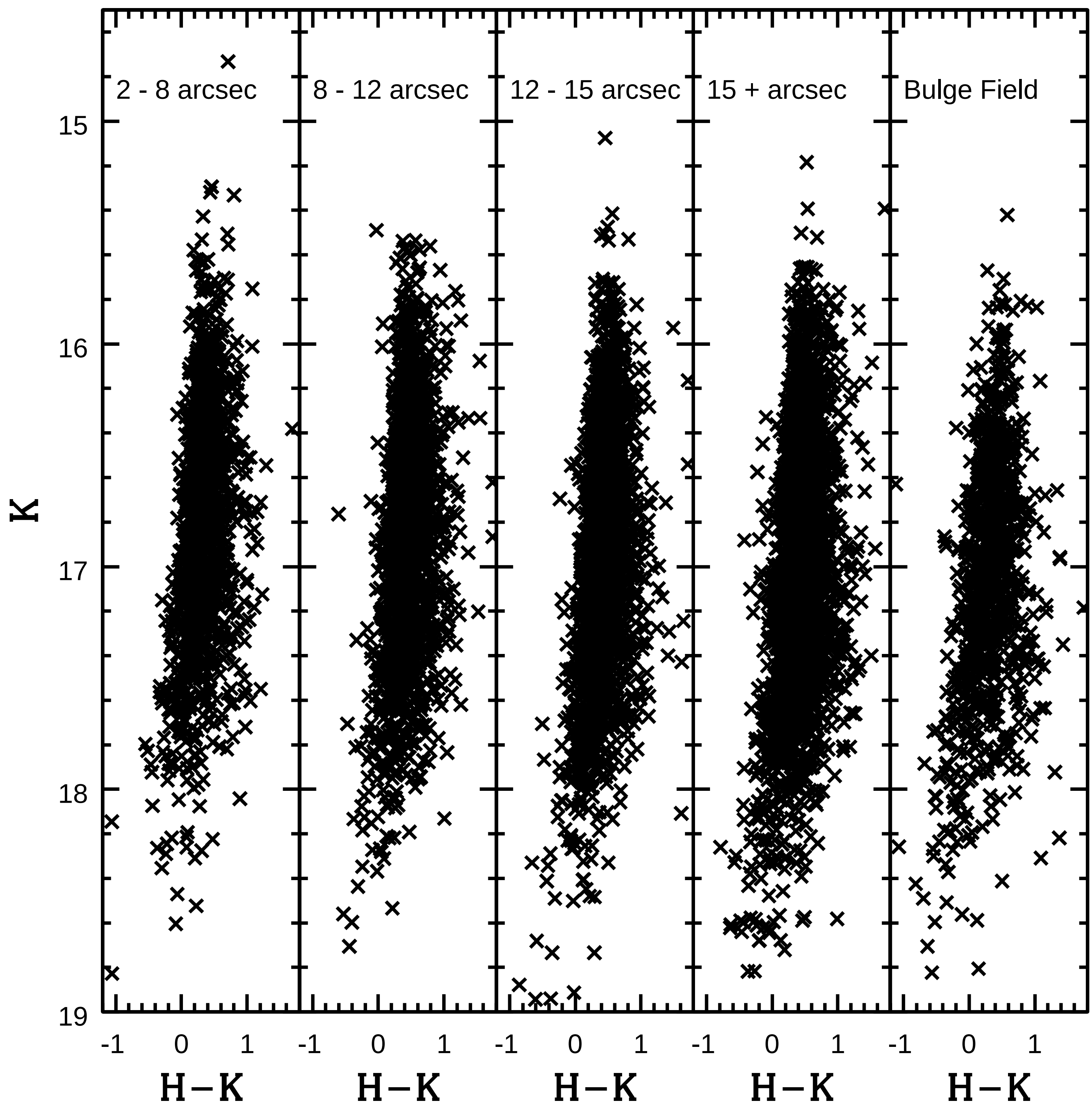

2 - 8 arcsec
8 - 12 arcsec
12 - 15 arcsec
15 + arcsec
Bulge Field
K
15
16
17
18
19
-1
0
1
H-K

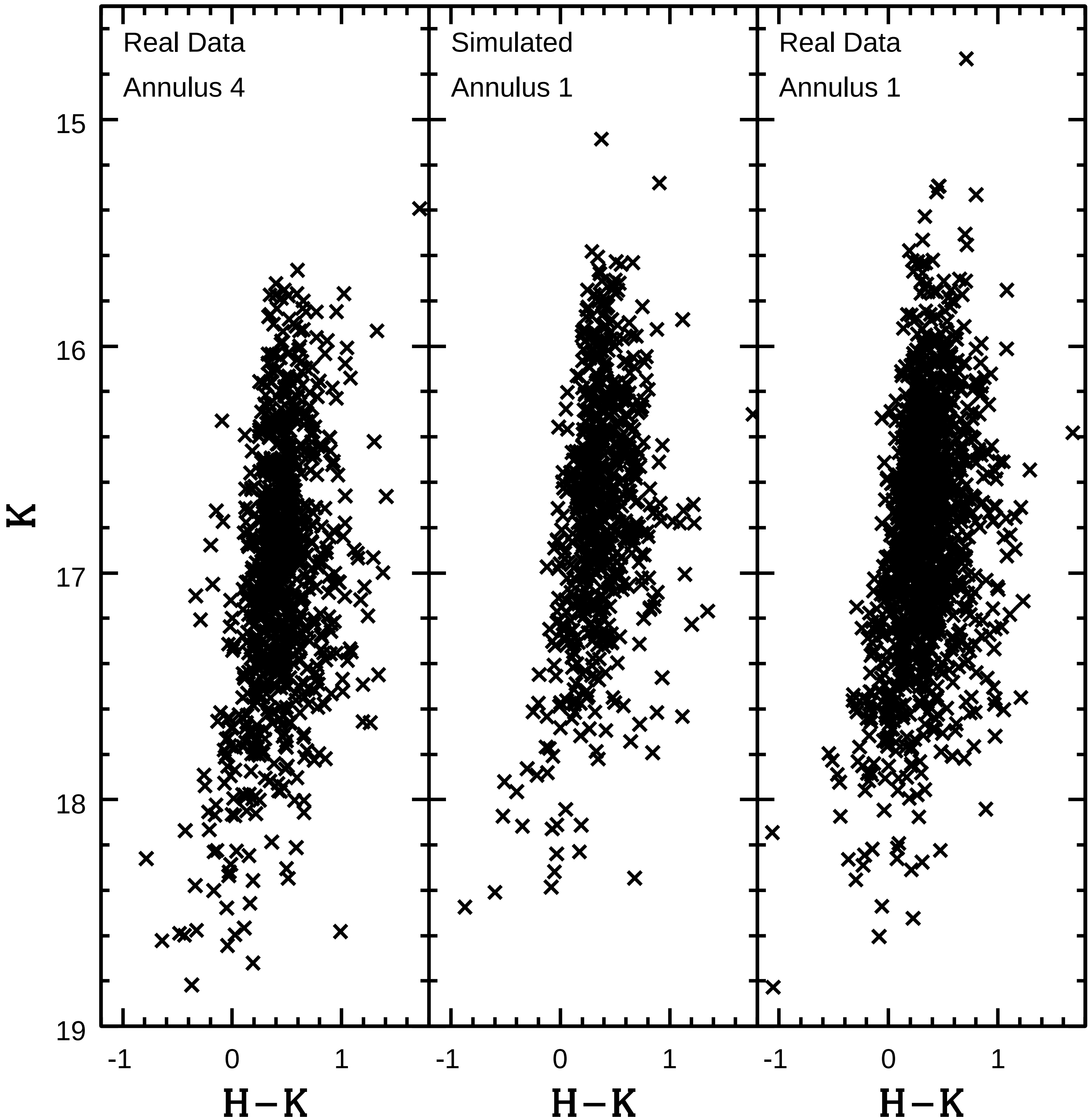
Real Data
Annulus 4
Simulated
Annulus 1
Real Data
Annulus 1
K
H−K
H−K
H−K
15
16
17
18
19
-1
0
1

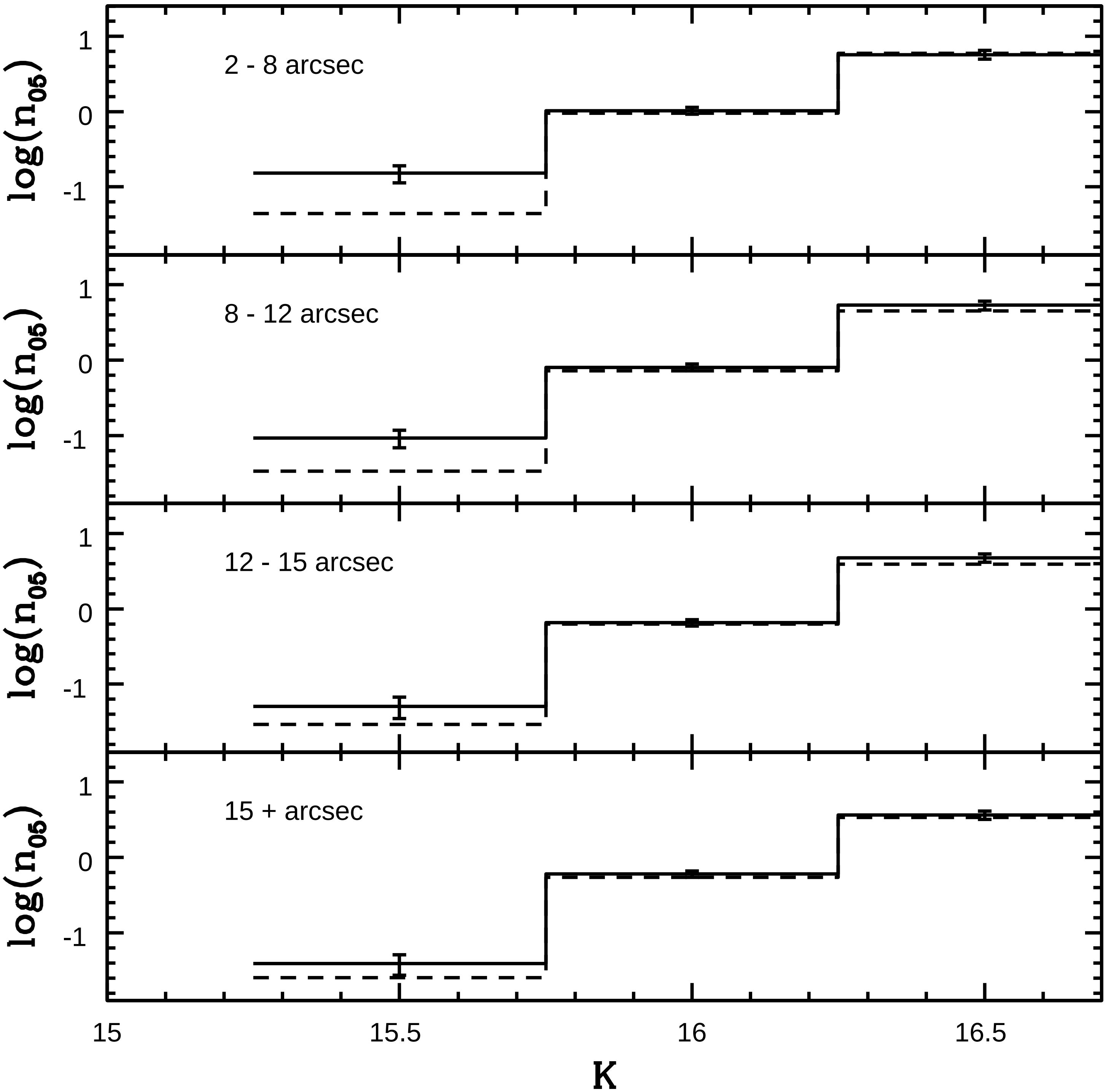

2 - 8 arcsec
8 - 12 arcsec
12 - 15 arcsec
15 + arcsec
log(n05)
1
0
-1
15
15.5
16
16.5
K

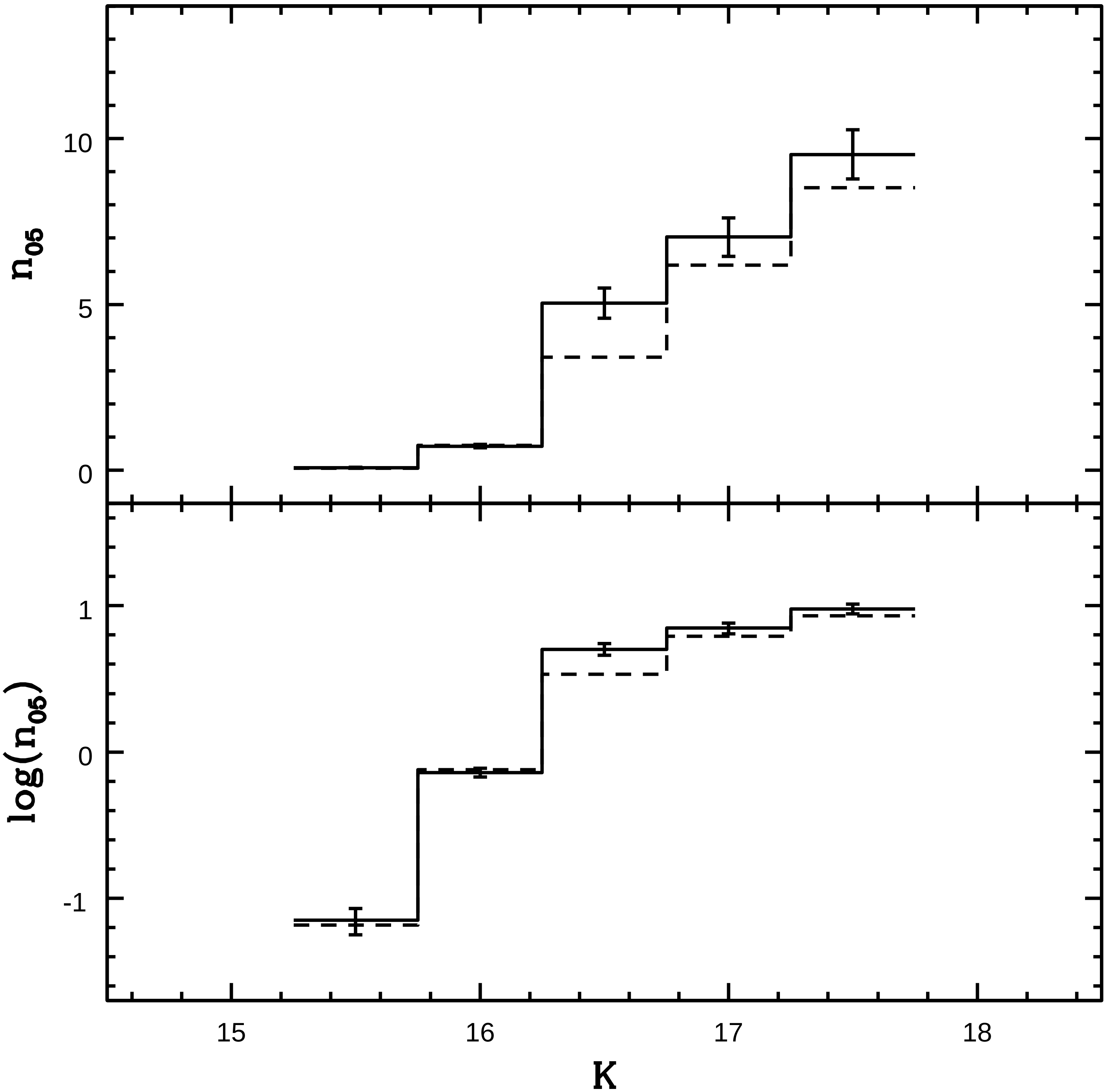

10
5
0
n_{05}
1
0
-1
$\log(n_{05})$
15
16
17
18
K